ADVANCED OPTICAL MATERIALS
www.advopticalmat.de

Thermal Runaway of Silicon-Based Laser Sails

Gregory R. Holdman, Gabriel R. Jaffe, Demeng Feng, Min Seok Jang, Mikhail A. Kats, and Victor W. Brar*

Laser sail-based spacecraft—where a powerful Earth-based laser propels a lightweight outer-space vehicle—have been recently proposed by the Breakthrough Starshot Initiative as a means of reaching relativistic speeds for interstellar space travel. The laser intensity at the sail required for this task is at least 1 GW m^{-2} and, at such high intensities, thermal management of the sail becomes a significant challenge even when using materials with low linear absorption coefficients. Silicon is proposed as one leading candidate material for the sail due to its low sub-bandgap absorption and high index of refraction, which allows for low-mass-density designs. However, here it is shown that the temperature-dependent linear absorption of silicon can lead to thermal runaway at temperatures above 400–500 K for even the most optimistic viable assumptions of the material quality. Additionally, above a design-specific threshold laser intensity, nonlinear two-photon absorption triggers thermal runaway regardless of initial temperature. Resonator-based designs, which concentrate the field, exhibit lower threshold intensities than geometries that minimize the electric field such as Bragg reflectors.

1. Introduction

Sending probes to nearby star systems requires engineering spacecraft that can travel at relativistic speeds. Recently, the Breakthrough Starshot Initiative has proposed to design, construct, and launch "laser sails" in order to achieve this goal, with an aim of sending a spacecraft toward Alpha Centauri at 20% the speed of light.[1] The proposed propulsion mechanism for these vehicles is radiation pressure from a ground-based laser array on a reflective "sail." Many design challenges must be overcome before such a project can be realized, and amongst the forefront of them is designing the sail, which must have high reflectivity, low mass, low absorption, lateral and rotational stability, and thermal stability. Optical metasurfaces and photonic crystals are ideally suited structures for laser sails because they can be made highly reflective,[2] have low areal densities,[3] and with the appropriate design can achieve self-correcting stability when accelerated by a high-powered optical beam.[4,5] However, absorption of even a tiny fraction of the incoming laser radiation, which will be on the order of 10 GW m^{-2}, poses major issues for sail thermal management because thermal radiation is the only passive mechanism for cooling in space. To prevent the sail from melting, it is crucial to choose materials that balance exceptionally low absorption coefficients at the drive laser wavelength in the near infrared (including the Doppler shift after the sail has accelerated) and high absorption coefficients in the mid-infrared to far infrared to increase radiative cooling.[3,6]

Silicon and silicon dioxide have emerged as two of the most attractive materials for laser sail designs based on metasurfaces, owing to the large contrast in their refractive indices, low material absorption at some of the proposed driving laser wavelengths ($\lambda_0 > 1.2$ μm),[3] low mass densities, and potential for fast integration with existing industrial silicon fabrication infrastructure.[6,7] In particular, one study of optimized sail structures found that a 1D Si grating provided superior acceleration performance over any SiN_x metasurface.[8] Previous studies of Si/SiO_2 sails—where the SiO_2 is utilized for radiative cooling—with anywhere from 25 to 400 GW m^{-2} incident laser intensity have predicted equilibrium temperatures below the melting points of the constituent materials assuming that the absorption coefficient of both materials is $< 10^{-2}$ cm^{-1}.[6,7] Furthermore, one of these works approached the design of the laser sail as a multiphysics problem taking into account not only thermal stability, but also mechanical stability of the sail in the beam.[7] However, these works did not take into account two important factors that can significantly affect the thermal stability of the sail. First, silicon exhibits a strong temperature-dependent absorption coefficient due to bandgap narrowing that, for example, at a temperature of 800 K and wavelength of 1.55 μm, can reach >4.5 cm^{-1}.[9] This value is ≈6 orders of magnitude higher than at room temperature.[10] Second, two-photon absorption (TPA) introduces additional absorption in

G. R. Holdman, G. R. Jaffe, V. W. Brar
Department of Physics
University of Wisconsin-Madison
1150 University Ave, Madison, WI 53706, USA
D. Feng, M. A. Kats
Department of Electrical and Computer Engineering
University of Wisconsin-Madison
Madison, WI 53706, USA
E-mail: mkats@wisc.edu
M. S. Jang
School of Electrical Engineering
Korea Advanced Institute of Science and Technology
Daejeon 34141, Korea
The ORCID identification number(s) for the author(s) of this article can be found under https://doi.org/10.1002/adom.202102835.

DOI: 10.1002/adom.202102835

silicon with a TPA coefficient of β =1.35 cm GW^{-1} at 1550 nm, which would cause the absorption of the sail to increase with laser power even at low temperatures.[11] For laser-phased arrays operating at intensities on the order of $I_0 \approx 10$ GW m^{-2}, TPA adds about 1.35×10^{-3} cm^{-1} to the absorption coefficient of Si, well above any absorption measured in Si at room temperature for low laser intensities. In this work, we show that these two properties can cause thermal instabilities in the sail during its acceleration phase.

To investigate the limits of thermal stability, we analyzed a Si/SiO_2-based metasurface laser sail that is designed to have a reflection coefficient of >99% at the laser wavelength of 1.55 µm and that exhibits a low areal mass density of <1 g m^{-2}.[1] In order to model the thermal characteristics of the sail, we assembled detailed models of the spectral and temperature-dependent absorption coefficients of both Si and SiO_2 from literature sources and used these in our simulations. We then used full-wave, finite element simulations to calculate the temperature dependence of the emissivity and absorptivity, and balanced these two factors to determine the stable sail temperature. We found that, even when using the lowest absorption coefficients ever demonstrated on the wafer scale, this metasurface sail has no equilibrium temperature for laser intensities $I_0 > 4.8$ GW m^{-2}. The mechanisms behind this are TPA at low temperatures and free-carrier absorption augmented by a decreasing bandgap at high temperatures, both in Si. For laser intensities $I_0 < 4.8$ GW m^{-2} we found that the sail can exhibit a stable equilibrium temperature, but fluctuations above a higher unstable equilibrium temperature could lead to thermal runaway regardless. While any Si/SiO_2 sail will exhibit this behavior, we demonstrate that a design which lowers the electric field in the Si, and therefore reduces the total absorption, can provide significant improvements to this limit.

2. Sail and Material Models

A schematic of the metasurface laser sail design used in this work is shown in **Figure 1**. Our Si/SiO_2-based metasurface

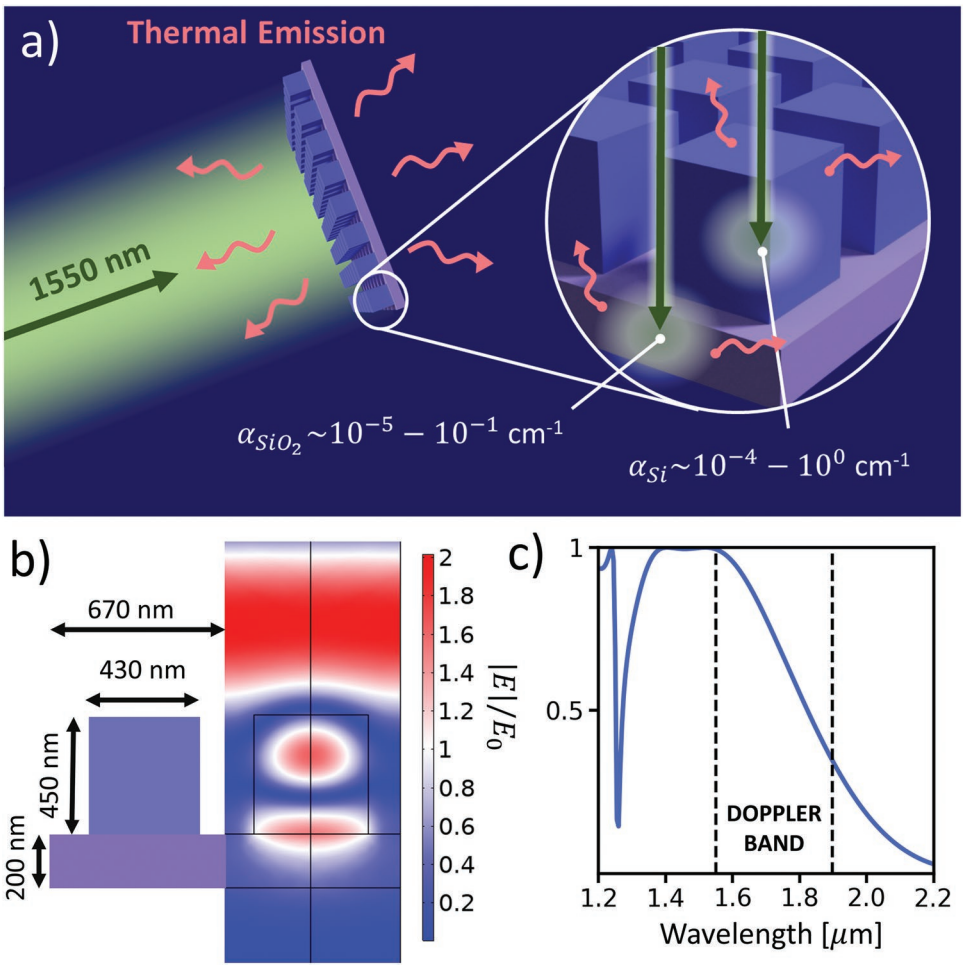

Figure 1. a) Laser sail probe being accelerated toward Alpha Centauri. Laser light is absorbed in the structure, which can only cool via thermal emission. Absorption coefficients at 1.55 µm are labeled. There is wide variability in these materials for different material quality, temperatures, and light intensities. b) Diagram of the metasurface used in this work consisting of 430-nm-wide by 450-nm-tall Si blocks (dark blue) with a pitch of 670 nm on a 200-nm-thick SiO_2 substrate (light purple). The colormap shows the electric field magnitude within the structure normalized to the incoming 1550 nm laser intensity. Note that field enhancement within the resonator causes the field intensity to exceed that of the incoming plane wave in localized regions. c) Reflection spectrum of the metasurface.

consists of 430-nm-wide by 450-nm-tall Si blocks on a 200-nm-thick SiO_2 substrate, with a total areal mass density of 0.96 g m^2. This structure is based on a previously published broadband perfect reflector geometry that uses Mie resonances to achieve perfect reflection.[2] For this work, we have re-optimized that structure to account for a finite-thickness silica layer, and achieved a reflectivity of 99.5% at a driving laser wavelength λ_0 =1550 nm and >95% from 1350 to 1605 nm.

Our simulations included models of the complex refractive indices of both materials. We assumed a constant real refractive index of $\mathrm{Re}[n_{Si}] = 3.42$ for Si because the index varies very little over the wavelength range of interest of 1–100 µm. The real part of the refractive index of SiO_2 $\mathrm{Re}[n_{SiO_2}]$ has been extensively studied.[12] The imaginary parts of the refractive indices require more care. In order to calculate the equilibrium temperature of a laser-heated Si/SiO_2 metasurface sail, comprehensive models of the temperature and wavelength dependence of the Si and SiO_2 absorption coefficients $\alpha = 4\pi\mathrm{Im}[n]/\lambda$ are needed. These models must be valid in the range of the expected equilibrium temperatures spanning 50–800 K, and cover both the Doppler-broadened laser wavelength range of 1.55–1.90 µm and the bandwidth of the thermal emission from 2 to 100 µm. We found no single literature source that provided absorption values over such a broad range of wavelengths and temperatures. We therefore assembled a composite absorption model for each material from multiple literature sources.

Our model can be seen in **Figure 2**. There are four different processes that contribute to the infrared absorption of Si. The total absorption, $\alpha_{\mathrm{Tot}}(\lambda, T, I)$, at a particular wavelength λ, temperature T, and local intensity $I = c\varepsilon_0|E|^2/2$, can be modeled as the sum of the absorption contributions from each absorption mechanism as

$$\alpha_{\mathrm{Tot}}(\lambda,T,I) = \alpha_{\mathrm{BG}}(\lambda,T) + \alpha_{\mathrm{FC}}(\lambda,T) + \alpha_{\mathrm{TPA}}(\lambda,I) + \alpha_{\mathrm{L}}(\lambda) \quad (1)$$

Here, α_{BG} is the coefficient of the bandgap absorption caused by the excitation of electrons in the valence band into the conduction band, and α_{FC} is the coefficient of the free-carrier absorption, which involves the transfer of photon energy to thermally excited free carriers in conduction or valence bands. The TPA coefficient is α_{TPA}, and α_{L} is the coefficient for the lattice absorption through multiphonon processes.

The composite absorption model for Si that we developed includes tabulated values of the total absorption coefficient between 0.25 and 1.45 µm,[13] a free-carrier absorption model spanning 1.45–5 µm,[9] and a second free-carrier model for the range of 4–100 µm[14] for which we assume the intrinsic-carrier concentration follows the model of Couderc et al.[18] We also include the multiphonon absorption bands from 7 to 100 µm[15,16] as well as tabulated coefficients for TPA which has a broad step near 2 µm.[11] The TPA process is a particularly important mechanism to consider when modeling metasurfaces designed to operate at high intensities. In Si at 300 K, the TPA at 1.55 µm is greater than the combined free-carrier and single-photon bandgap absorption for fluences >900 kW m^{-2}. Further information regarding interpolation between models and the fits to the multiphonon modes is available in the Supporting Information.

The amorphous SiO_2 absorption model we assembled includes the extensive collation of room-temperature wavelength-dependent absorption measurements of SiO_2 glass in the range 0.015–100 µm.[12] The room-temperature values are used at all sail temperatures in our models because the absorption of SiO_2 exhibits only a weak temperature dependence from 300 to –1100 K between 1 and 7 µm.[19–21] We note that the growth conditions, defect density, and concentration of hydroxyl groups are known to have a strong effect on the absorption of SiO_2 in the infrared and are responsible for the significant variation in the reported absorption of SiO_2 at 1.55 µm. Films of SiO_2 grown via wet oxidation of Si followed by a 24 h dry oxidation at 1000 °C have demonstrated absorption as low as 4.1×10^{-5} cm^{-1} on the wafer scale.[17] This absorption value is three orders of magnitude smaller than the typical value of 2.4×10^{-2} cm^{-1}.[12] Even lower values of absorption have been demonstrated in optical fibers, but have yet to be realized at the wafer scale. We refer to the above absorption coefficients at 1.55 µm as "Hero" and "Typical," respectively, and they are denoted in Figure 2 by grey diamonds. To our knowledge, the "Hero" ultra-low SiO_2 absorption has only been demonstrated in a single experiment.

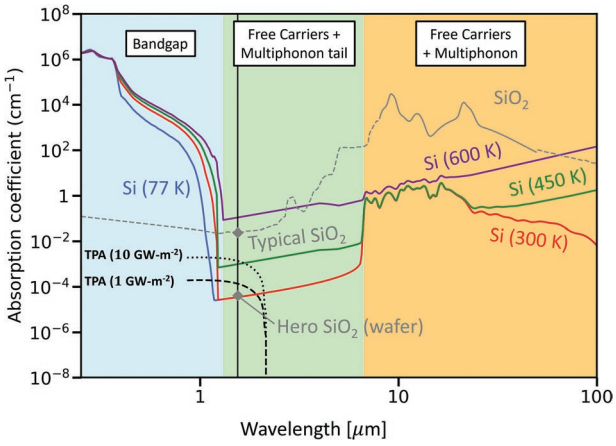

Figure 2. A composite model from multiple literature sources of the absorption coefficient of Si as a function of wavelength at various temperatures (colored lines) and amorphous SiO_2 at room temperature (grey line).[12] The blue, green, and orange shaded regions indicate the dominant absorption mechanisms for each wavelength range for Si. The model is composed of bandgap absorption,[13] free-carrier absorption,[9,14] and multiphonon absorption.[15,16] TPA at intensities 1 and 10 GW m^{-2} are included as dashed black lines.[11] The data point labeled "Hero" indicates the lowest demonstrated absorption value of SiO_2 at a wavelength of 1.55 µm in a wafer.[17] The vertical line indicates the laser wavelength of 1.55 µm. Further details regarding the Si composite absorption model are available in the Supporting Information.

3. Simulation of Metasurface Thermal Balancing

During the acceleration phase, the sail absorbs energy from the driving laser while the only mechanism for losing energy is thermal radiation. The absorbed laser power will raise the temperature of the sail until it reaches an equilibrium temperature T_i, at which point the absorbed intensity I_A and thermally

emitted intensity I_E are equal. Perturbations may drive the sail above or below T_i, but if a rising temperature causes $I_E(T)$ to exceed $I_A(T)$, the equilibrium temperature will be stable because excess emission cools the sail. Likewise if $I_A(T)$ increases above $I_E(T)$ with T, then T_i is an unstable equilibrium as the sail absorbs more energy than it can emit and it undergoes thermal runaway. It is possible that $I_A(T) > I_E(T)$ for a large range, possibly even all values of T. In this case, the temperature will increase until the sail melts or is otherwise destroyed. In this work, we predicted the equilibrium temperatures of the sail in Figure 1a by calculating $I_A(T)$ and $I_E(T)$ for a large range of temperatures and then identified the T_i where $I_A(T_i) \approx I_E(T_i)$.

We computed the quantities $I_A(T, I_0)$ and $I_E(T)$ in different ways. Absorbed intensity $I_A(T, I_0)$ at the driving laser wavelength 1.55 μm was calculated by using a full-wave FDTD simulation (Ansys Lumerical) to obtain the local field distribution, exporting the data, and performing the following volumetric integration

$$I_A(T, I_0) = \frac{\omega_0}{A} \int \mathrm{Im}\{\varepsilon[\omega_0, T, I(\mathbf{r})]\} |E|^2 \, dV \tag{2}$$

where A is the area of the unit cell, $\omega_0 = 2\pi c/\lambda_0$, ε is the permittivity of the constituent materials, and $I(\mathbf{r})$ is the local intensity. The permittivity acquires a dependence on $I(\mathbf{r})$ in the Si due to TPA. For $I_E(T)$, it is computationally challenging to calculate the exact thermal emission of the metasurface structure using full-wave simulations given that light is emitted over a broad bandwidth (λ ~2–100 μm), over all angles, and with both s and p polarizations. Thus, to calculate $I_E(T)$, we approximated the Si layer as a material with an effective index $n_{\mathrm{eff}} = F \times n_{Si}$ where $F = 430^2/670^2 \approx 41\%$ is the fill factor of the Si in our metasurface design, and n_{Si} is the bulk Si refractive index. This approach leverages the fact that the characteristic length scale of the metasurface is much smaller than the emission wavelengths. We confirmed the validity of this method by comparing full-wave simulations of the metasurface to the approximated structure for a few chosen angles (see Supporting Information). We then implemented a transfer matrix method to calculate reflection and transmission which were used to derive absorptivity $A = 1 - R - T$.[22] Emissivity was then calculated via Kirchhoff's law of thermal radiation, equating emissivity to absorptivity, and the overall thermal emission was calculated by integrating over the Planck distribution in wavelength, angle, and polarization.[23]

Figure 3a–c displays $I_A(T, I_0)$ and $I_E(T)$ for the total structure as well as the constituent materials. At all temperatures, SiO_2 dominates thermal emission and roughly follows a T^4 power law. When the metasurface is made with Hero SiO_2, an incident intensity of I_0 = 1 GW m^{-2} yields two equilibrium temperatures of 189 and 512 K with the former being stable and the latter unstable. Above 512 K, thermal runaway occurs as the sail absorbs more energy than it can emit. Increasing the incident intensity to I_0 = 10 GW m^{-2}, we found no equilibrium temperature exists in Hero SiO_2, and thermal runaway occurs at all temperatures. For metasurfaces using Typical SiO_2 and I_0 = 1 GW m^{-2}, the SiO_2 absorption dominates over the TPA in Si at low temperatures. We found that the stable and unstable equilibrium temperatures are very close at 423 and 477 K. This means a small fluctuation in incident intensity could put the sail into the thermal runaway region and cause it to melt. Figure 3d displays the difference in emissive intensity I_E and absorptive intensity I_A as a function of both T and I_0 for the case of Hero SiO_2. There is a large region where this value is positive indicating the sail will cool to the stable equilibrium temperature, provided the initial temperature is below the unstable equilibrium temperature. We found that no stable equilibrium temperature exists for $I_0 > 4.8$ GW m^{-2} implying that the temperature will increase until it melts, evaporates, or otherwise fails.

The existence of a maximum laser intensity set by the thermal limits we calculate here also place limits on the maximum achievable acceleration of the sail. Laser sail designs in other works assumed $I_0 \approx 25$ GW m^{-2},[6,7] whereas our work demonstrates that a particular Si/SiO_2 metasurface sail will be limited to $I_0 < 4.8$ GW m^{-2} using the best materials available. A commonly used figure of merit for sail performance is the smallest possible acceleration distance (AD) for a given incident intensity and target speed.[3,8,24]

$$\mathrm{AD} = \frac{c^3}{2I_0} \rho \int_0^{\beta_f} \frac{h(\beta)}{R[\lambda(\beta)]} d\beta \tag{3}$$

where ρ is the sail areal density, $\beta = v/c$ is the velocity normalized to the speed of light, and $h(\beta) = \beta/(1-\beta)^2\sqrt{1-\beta^2}$ accounts for relativistic corrections. We assume a constant laser intensity I_0 and use the reflection spectrum in Figure 1c, along with the areal density, to calculate the AD for the sail studied here, which we found to be 26 Gm for a laser intensity of I_0 = 25 GW m^{-2}. However, using a thermally limited laser intensity of I_0 = 4.8 GW m^{-2} yields an AD of 148.9 Gm, a penalty of a factor of ≈6. We note that our metasurface sail was initially chosen to maximize reflectivity at 1550 nm, not minimize the AD. However, as shown in the Supporting Information, a rudimentary optimization of this design for minimal AD can be performed by scaling the dimensions proportionally. We find that increasing the dimensions by 5% yields a slightly lower AD of 126.5 Gm, largely due to increased reflectivity over the Doppler-shifted wavelength range of the laser. Alternative designs that maintain high reflectivity while minimizing the electric field concentration in the Si could potentially reduce AD further by allowing for higher laser intensities. This topic is explored further in the next section.

4. Thermal Balance of Bragg Reflector

As is clear from Figure 1b, the highly reflective metasurface we studied concentrates the incident field in the high index Si blocks. Considering that the two-photon nonlinear absorption in the Si scales as $|E|^4$, a design which concentrates the field outside of the Si would, theoretically, improve the thermal stability of the sail. A Bragg reflector, which operates by destructive interference of the electric field inside the structure, is an example of such a design.

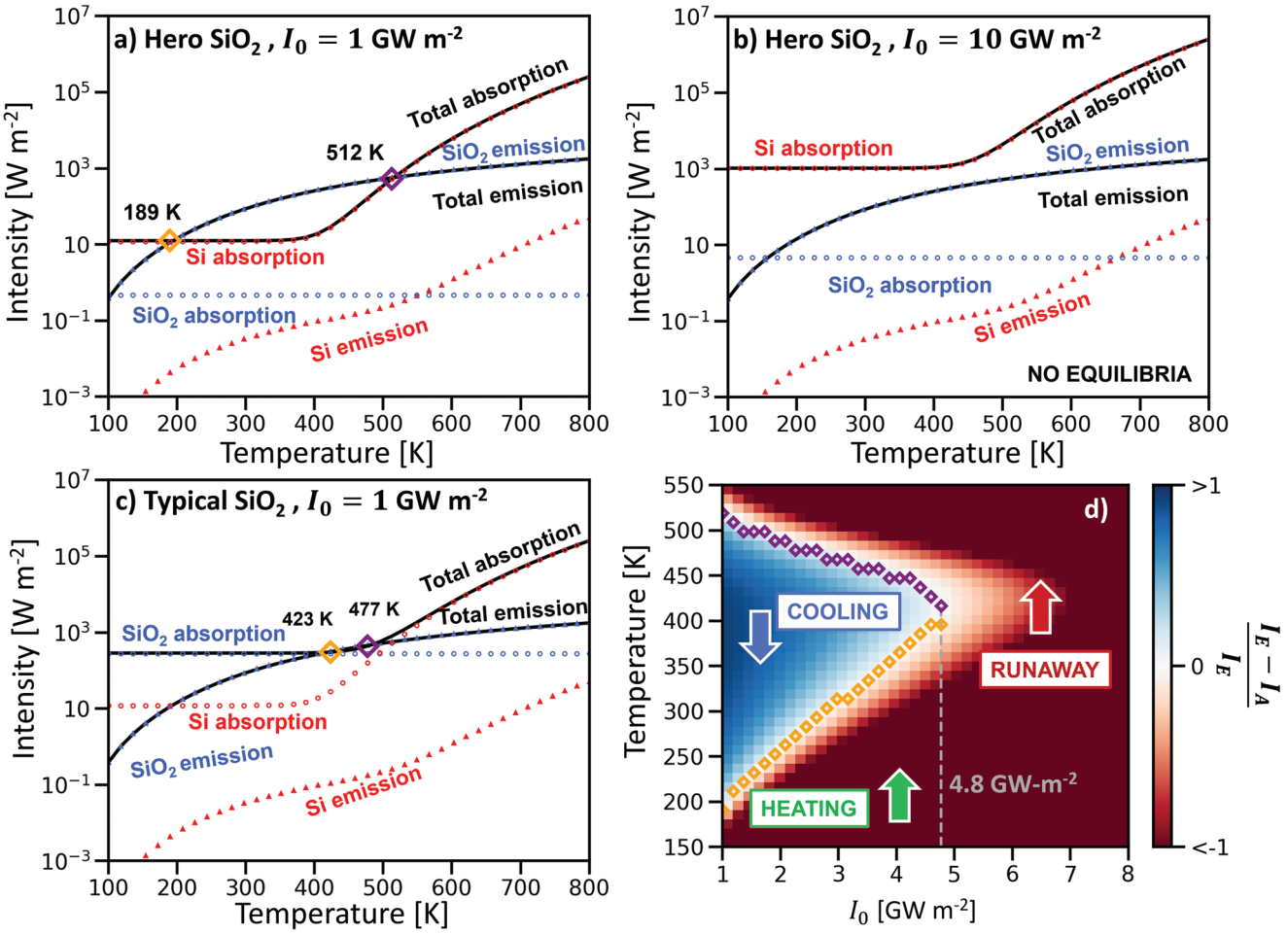

Figure 3. a–c) Absorbed and thermally emitted intensities versus temperature for the Si/SiO_2 metasurface depicted in Figure 1 made from either Hero or Typical SiO_2 and illuminated with an incident laser intensity I_0. Stable (orange) and unstable (purple) equilibrium temperatures are labeled as diamonds. Note that there is no equilibrium temperature for Hero SiO_2 at I_0 =10 GW m^{-2}. Absorbed and emitted intensities for the complete laser sail are shown in black while the contribution of the Si and SiO_2 layers are shown in red and blue, respectively. Dotted lines are used to indicate the Si absorption and SiO_2 emission because they overlap with the total absorption and emission. d) Normalized difference in emissive intensity and absorptive intensity as a function of temperature T and incident intensity I_0 for a sail made with Hero SiO_2. Stable and unstable equilibrium temperatures are indicated as orange and purple diamonds, respectively. The blue and green arrows indicate the zones where the sail will either cool or heat to a stable equilibrium temperature below $I_0 \approx 4.8$ GW m^{-2}. Otherwise, thermal runaway occurs.

In order to explore the comparative thermal stability of Bragg reflectors to dielectric metasurfaces we modeled Bragg reflector structures that consist of alternating layers of Si and SiO_2 of thicknesses 113.3 and 269.1 nm, respectively, corresponding to the quarter wavelength condition for 1550 nm light. The electric field magnitude of normally incident 1550 nm light is shown in **Figure 4**a for one to four layers of Si/SiO_2. In contrast to the metasurface, the Bragg reflector reduces rather than concentrates the field. Each successive layer also reduces the field by roughly an order of magnitude, so extra layers will not significantly add to the total absorption. The reflection spectrum is sufficiently broadband (Figure 4b) and increases with the number of layers. Thus, the Bragg reflector is a strong candidate for providing low values of AD by allowing for large incident laser intensities.

We calculate the maximum intensity I_{Max} and resulting AD for one to four layers using the methods described in the previous section. An example of the calculation of I_{Max} for one layer is shown in Figure 4c. Our results are shown in **Table 1**. Increasing the number of layers raises the areal mass density proportionally while only slightly raising I_{Max} and reflection. We therefore find that one layer is optimal providing an AD of 18.4 Gm.

We note that while the Bragg reflector improves the performance of Si/SiO_2 sails in terms of AD, this is achieved by allowing for order of magnitude larger laser intensities, which would significantly raise the overall cost of the project. In fact, the optimal single layer Bragg design is only ≈50% reflective, and would waste large amounts of power. Moreover, a Bragg reflector design would not be compatible with passive stability schemes that are possible with metasurface sails[4,5,25,26] and would not enable the use of flat optics for focusing of communication lasers to relay signals back to Earth, as has been proposed.[4]

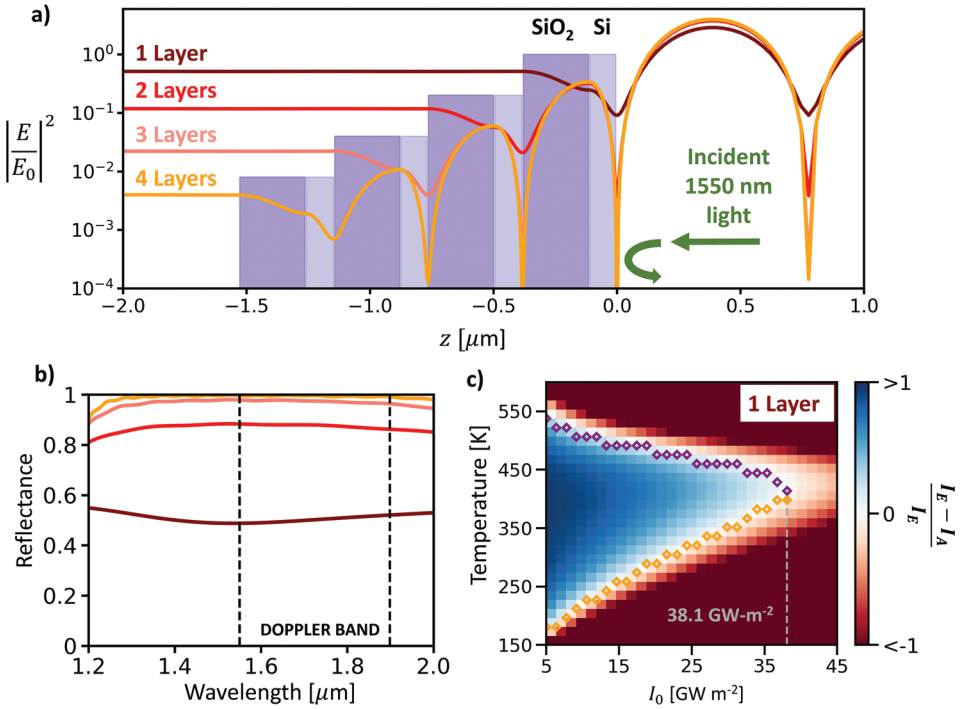

Figure 4. a) Side view of Bragg reflector showing electric field magnitude normalized to incident field $|E/E_0|^2$ as a function of distance above surface of Bragg reflector for various numbers of layers. Silicon and silicon dioxide are 113.3 and 269.1 nm thick, respectively. b) Reflection spectra of Bragg stacks for various numbers of layers. Red corresponds to the Doppler band. c) Normalized difference in emissive intensity and absorptive intensity as a function of temperature T and incident intensity I_0 for single layer Bragg reflector made with Hero SiO_2.

5. Discussion

The thermal runaway of the sails that we predict at high temperatures is caused by the increasing free-carrier absorption of Si with temperature, because the bandgap of Si shrinks and the population of thermally excited carriers increases. At low temperatures, if the low-loss Hero SiO_2 is used, TPA in Si dominates the absorption of the sail. Since TPA increases linearly with incident power, the absorbed power of the sail increases with the square of the incident power, that is, $I_A \propto I_0^2$. Strong TPA at low temperatures is sufficient to raise the temperature of the sail to the point where the increasing free-carrier and bandgap absorption cause a thermal runaway. In principle, it would be possible to avoid TPA by choosing a laser wavelength longer than 2 μm, but phonon-mediated absorption in both Si and SiO_2 will increase, as will free-carrier absorption in the Si. Detailed modeling beyond 2 μm, however, is inhibited by a lack of absorption data in Hero-quality SiO_2 and Si at those wavelengths. Below 2 μm, all laser sail designs containing Si must contend with TPA. Through the Bragg reflector example, we have shown that one approach to solving the thermal runaway problem may be to use a sail design that concentrates the electric field outside of the Si layer.

Table 1. Resulting areal mass density, I_{Max}, and AD for various numbers of layers of the Bragg reflector.

Layers	Density [g m^{-2}]	I_{Max} [GW m^{-2}]	AD [Gm]
1	0.98	38.1	18.4
2	1.96	39.5	20.7
3	2.94	40.9	27.0
4	3.92	43.6	33.0

Our work provides an optimistic upper bound on the maximum intensity I_{Max} that a Si-based sail could survive. There are other effects that could increase the absorption of the sail, further reducing this maximum survivable intensity. For instance, strain is known to decrease the bandgap of silicon, which will significantly increase absorption at the proposed laser wavelengths.[27] In addition, dangling bonds at defects in Si exhibit strong absorption peaks in the mid-infrared.[28] There is also the danger that small localized transient temperature fluctuations, caused by impact events with gas molecules and dust, could lead the entire sail into thermal runaway.[29]

The total emission of the sail could be increased to counteract the effects of TPA. Laser cooling using rare-earth ions,[30] nanoparticle laminate films,[31] and multiscale segmented designs[32] have also been proposed. Additionally, the emission spectrum of coupled resonators has been shown to be highly tunable,[33] and such techniques could be applied to increase the emission of a sail incorporating SiO_2.

It is possible that light sails constructed of a different material, such as SiN_x, would not exhibit the thermal runaway behavior of Si sails. However, detailed studies of the absorption behavior of most materials at high laser intensities and high temperatures, including SiN_x, are lacking. In the case of Si_3N_7, TPA has been shown to be negligible at 1550 nm, yet exceeds that of Si at 1060 nm, another potential driving laser

wavelength.[34] Additionally, some materials could exhibit effects not seen in Si, like stoichiometric instabilities, which could also lead to similar thermal runaway behavior despite reduced free-carrier absorption and bandgap narrowing effects.[35] Thus, our results highlight the need to measure the optical constants of all candidate materials with ppm sensitivity in high-temperature and high-intensity conditions where nonlinearities can occur.

We note that the constraints outlined in this work are emergent effects that occur at high laser intensities, and thus do not eliminate Si/SiO_2 solar sails from being constructed.[29] In addition, the intensity constraint is well below the threshold needed for interplanetary laser sail missions.[1]

6. Conclusion

In this work, we demonstrated that a Si/SiO_2 metasurface floating in vacuum and exposed to a 1.55 µm laser with an intensity above a threshold I_{Max} will melt, regardless of starting temperature. Equilibrium temperatures will exist at lower incident laser intensities; however, a thermal runaway process will melt the sail if the sail temperature reaches the 400–500 K range. The use of high-quality SiO_2 with low absorption will increase the thermal stability of the sail to a point, but ultimately the absorption will be dominated by two-photon absorption (TPA) in Si. Thus, the potential for thermal runaway must be taken into account when designing a laser sail that incorporates a material with temperature-dependent absorptivity such as Si. It is possible that other candidate materials for the Breakthrough Starshot Initiative project could exhibit this behavior as well. Where the data is not available in the literature, measurements must be performed to characterize the materials.

Supporting Information

Supporting Information is available from the Wiley Online Library or from the author.

Acknowledgements

G.R.H. and G.R.J. contributed equally to this work. This work was supported by the Breakthrough Initiatives, a division of the Breakthrough Prize Foundation, and by the Gordon and Betty Moore Foundation through a Moore Inventors Fellowship.

Conflict of Interest

The authors declare no conflict of interest.

Data Availability Statement

The data that support the findings of this study are available in the Supporting Information of this article.

Keywords

laser propulsion, laser sail, metasurfaces, thermal management

Received: December 29, 2021
Revised: May 8, 2022
Published online: July 18, 2022

[1] Breakthrough initiatives, https://breakthroughinitiatives.org/initiative/3 (accessed: November 2021).
[2] B. Slovick, Z. G. Yu, M. Berding, S. Krishnamurthy, *Phys. Rev. B* **2013**, *88*, 165116.
[3] H. A. Atwater, A. R. Davoyan, O. Ilic, D. Jariwala, M. C. Sherrott, C. M. Went, W. S. Whitney, J. Wong, *Nat. Mater.* **2018**, *17*, 861.
[4] J. Siegel, A. Y. Wang, S. G. Menabde, M. A. Kats, M. S. Jang, V. W. Brar, *ACS Photonics* **2019**, *6*, 2032.
[5] O. Ilic, H. A. Atwater, *Nat. Photonics* **2019**, *13*, 289.
[6] O. Ilic, C. M. Went, H. A. Atwater, *Nano Lett.* **2018**, *18*, 5583.
[7] M. M. Salary, H. Mosallaei, *Laser Photonics Rev.* **2020**, *14*, 1900311.
[8] W. Jin, W. Li, M. Orenstein, S. Fan, *ACS Photonics* **2020**, *7*, 2350.
[9] H. Rogne, P. J. Timans, H. Ahmed, *Appl. Phys. Lett.* **1996**, *69*, 2190.
[10] J. Degallaix, R. Flaminio, D. Forest, M. Granata, C. Michel, L. Pinard, T. Bertrand, G. Cagnoli, *Opt. Lett.* **2013**, *38*, 2047.
[11] A. D. Bristow, N. Rotenberg, H. M. van Driel, *Appl. Phys. Lett.* **2007**, *90*, 191104.
[12] R. Kitamura, L. Pilon, M. Jonasz, *Appl. Opt.* **2007**, *46*, 8118.
[13] M. A. Green, *Sol. Energy Mater. Sol. Cells* **2008**, *92*, 1305.
[14] D. K. Schroder, R. N. Thomas, J. C. Swartz, *IEEE J. Solid-State Circuits* **1978**, *13*, 180.
[15] F. A. Johnson, *Proc. Phys. Soc.* **1959**, *73*, 265.
[16] E. J. Wollack, G. Cataldo, K. H. Miller, M. A. Quijada, *Opt. Lett.* **2020**, *45*, 4935.
[17] H. Lee, T. Chen, J. Li, K. Y. Yang, S. Jeon, O. Painter, K. J. Vahala, *Nat. Photonics* **2012**, *6*, 369.
[18] R. Couderc, M. Amara, M. Lemiti, *J. Appl. Phys.* **2014**, *115*, 093705.
[19] O. J. Edwards, Optical absorption coefficients of fused silica in the wavelength range 0.17 to 3.5 microns from room temperature to 980 °C, Technical Note D-3257, NASA, Washington, D.C. **1966**.
[20] A. Dvurechensky, V. Petrov, V. Yu Reznik, *Infrared Phys.* **1979**, *19*, 465.
[21] C. Tan, J. Arndt, *J. Phys. Chem. Solids* **2000**, *61*, 1315.
[22] J. E. Sipe, *J. Opt. Soc. Am. B* **1987**, *4*, 481.
[23] D. G. Baranov, Y. Xiao, I. A. Nechepurenko, A. Krasnok, A. Alú, M. A. Kats, *Nat. Mater.* **2019**, *18*, 920.
[24] N. Kulkarni, P. Lubin, Q. Zhang, *Astron. J.* **2018**, *155*, 155.
[25] Z. Manchester, A. Loeb, *Astrophys. J.* **2017**, *837*, L20.
[26] G. A. Swartzlander, *J. Opt. Soc. Am. B* **2017**, *34*, C25.
[27] J. Cai, Y. Ishikawa, K. Wada, *Opt. Express* **2013**, *21*, 7162.
[28] W. B. Jackson, N. M. Johnson, D. K. Biegelsen, *Appl. Phys. Lett.* **1983**, *43*, 195.
[29] A. R. Davoyan, J. N. Munday, N. Tabiryan, G. A. Swartzlander, L. Johnson, *Optica* **2021**, *8*, 722.
[30] W. Jin, C. Guo, M. Orenstein, S. Fan, arXiv:2109.02702, **2021**.
[31] P. R. Wray, M. P. Su, H. A. Atwater, *Opt. Express* **2020**, *28*, 35784.
[32] J. Brewer, M. F. Campbell, P. Kumar, S. Kulkarni, D. Jariwala, I. Bargatin, A. P. Raman, *arXiv:2106.03558*, **2021**.
[33] A. M. Morsy, M. L. Povinelli, *Opt. Express* **2021**, *29*, 5840.
[34] B.-U. Sohn, J. W. Choi, D. K. T. Ng, D. T. H. Tan, *Sci. Rep.* **2019**, *9*, 10364.
[35] S. Singhal, *Ceramurgia Int.* **1976**, *2*, 123.